2021

Pomegranate (Punica granatum) extract and its polyphenols reduce the formation of methylglyoxal-DNA adducts and protect human keratinocytes against methylglyoxal-induced oxidative stress

Hao Guo

Chang Liu
University of Rhode Island, hichang813@uri.edu

Qi Tang
University of Rhode Island

Deyu Li
University of Rhode Island, deyuli@uri.edu

University of Rhode Island

See next page for additional authors

Citation/Publisher Attribution

Guo, H., Liu, C., Tang, Q., Li, D., Wan, Y., Li, J.-H.,...& Chen, H.-D. (2021). Pomegranate (*Punica granatum*) extract and its polyphenols reduce the formation of methylglyoxal-DNA adducts and protect human keratinocytes against methylglyoxal-induced oxidative stress. *Journal of Functional Foods, 83*, 104564. https://doi.org/10.1016/j.jff.2021.104564
Available at: https://doi.org/10.1016/j.jff.2021.104564

Journal of Functional Foods 83 (2021) 104564

Contents lists available at ScienceDirect

Journal of Functional Foods

journal homepage: www.elsevier.com/locate/jff

Pomegranate (*Punica granatum*) extract and its polyphenols reduce the formation of methylglyoxal-DNA adducts and protect human keratinocytes against methylglyoxal-induced oxidative stress

Hao Guo [a,b,c], Chang Liu [b], Qi Tang [b], Deyu Li [b], Yinsheng Wan [c], Jiu-Hong Li [a], Xing-Hua Gao [a], Navindra P. Seeram [b], Hang Ma [b,*], Hong-Duo Chen [a,*]

[a] Department of Dermatology, Key Laboratory of Immunodermatology, The First Hospital of China Medical University, Shenyang 110001, China
[b] Department of Biomedical and Pharmaceutical Sciences, College of Pharmacy, University of Rhode Island, Kingston, RI 02881, USA
[c] Department of Biology, Providence College, Providence, RI 02918, USA

ARTICLE INFO

Keywords:
Pomegranate (*Punica granatum*)
Punicalagin
Methylglyoxal
DNA damage
Wound healing
Skin protection

ABSTRACT

Pomegranate extract (PE) and its polyphenols have been reported to show skin protective effects but their cytoprotective effects against methylglyoxal (MGO)-induced DNA damage and cell dysfunctions are unclear. Herein, we evaluated whether PE, punicalagin (PA), ellagic acid (EA), and urolithin A (UA), can alleviate MGO-induced DNA damage in human keratinocytes. PE (50 μg/mL) and PA (50 μM) protected DNA integrity and reduced the formation of MGO-DNA adducts and tailed DNA by 60.2 and 49.7%, respectively, in HaCaT cells. PE and PA reduced MGO-induced cytotoxicity by increasing the cell viability (by 17.5 and 15.0%) and decreasing reactive oxygen species (by 28.3 and 30.0%), respectively. PE and PA also ameliorated MGO-induced cell dysfunction by restoring cell adhesion, migration, and wound healing capacity. Findings from this study provide insights into the skin protective effects of PE and its polyphenols supporting their applications as potential bioactive ingredients for cosmeceuticals.

1. Introduction

Reactive carbonyl species (RCS) are highly electrophilic compounds generated from the oxidation of carbohydrate (i.e. glucose), lipids, and amino acids (Mano, 2012). RCS interact with proteins or nucleic acids (i.e. DNA and RNA) via the Maillard reaction to form mis-folded macromolecule complexes known as advanced glycation endproducts (AGEs) (Singh, Barden, Mori, & Beilin, 2001). Therefore, RCS are considered as glycating agents and inducers of AGEs. During the formation of AGEs, carbohydrate metabolites can also be oxidized to generate RCS including reactive dicarbonyl chemicals, such as methylglyoxal (MGO). This positive feedback loop can lead to elevated RCS levels in living organisms, which is linked to various detrimental biological effects including DNA glycation and the induction of oxidative stress (Semchyshyn, 2014). For instance, MGO, a highly reactive electrophilic RCS, induces DNA glycation by attacking DNA nucleobase (i.e. guanine) to form MGO-DNA adducts including aminocarbinol (N^2-1-hydroxy-2-oxopropyl-guanine), carboxyethyl-deoxyguanosine (CEdG), and imidazopurinone [6,7-dihydro-6,7-dihydroxy-7-methyl-imidazo[2,3-b]purin-9(8)one] (Richarme et al., 2017). These MGO-DNA adducts mediate DNA glycation, which leads to several DNA damages including DNA strand breaks and replication mutation (Murata-Kamiya & Kamiya, 2001). Furthermore, high level of cellular MGO is often accompanied by elevated generation of reactive oxygen species (ROS), which is correlated with numerous detrimental effects, such as abnormal cell death and impaired cell functions. In addition, MGO-induced oxidative stress is linked to various diabetic skin complications including accelerated skin aging, skin dryness, and diabetic blisters and ulcer (Schalkwijk & Stehouwer, 2020). In particular, spiked RCS level in keratinocytes leads to impaired cell functions including undermined adhesion, migration, and wound healing abilities (Yang et al., 2014). Therefore, AGEs inhibitors with RCS scavenging capacity may be potential management strategies for AGEs-mediated diabetic skin complications. Phytochemicals from ethnomedicinal plants including pomegranate (*Punica*

Abbreviations: AGEs, advanced glycation endproducts; EA, ellagic acid; MGO, methylglyoxal; PA, punicalagin; PE, pomegranate extract; RCS, reactive carbonyl species; ROS, reactive oxygen species; UA, urolithin.

* Corresponding authors.
E-mail addresses: hang_ma@uri.edu (H. Ma), chenhd@cae.cn (H.-D. Chen).

https://doi.org/10.1016/j.jff.2021.104564
Received 17 December 2020; Received in revised form 26 May 2021; Accepted 27 May 2021
Available online 5 June 2021

granatum) have been reported to show anti-glycation effects (Kumagai et al., 2015; Kusirisin et al., 2009; Ramkissoon, Mahomoodally, Ahmed, & Subratty, 2013), which provide an attractive ethnomedicine-based intervention strategy for the potential prevention and treatment of AGEs mediated diabetic complications.

Our group's research efforts have been dedicated to the investigation of ethnomedicinal plants and functional foods for their inhibitory effects on the formation of AGEs (Liu et al., 2018, 2014Liu et al., 2017; Ma et al., 2018, 2015; Ma, Johnson, & et al., 2016; Sun et al., 2016; Zhang, Ma, Liu, Yuan, & Seeram, 2015). During the course of these projects, a series of natural products including botanical extracts and their phytochemicals were identified as AGEs inhibitors with MGO-trapping effects (Liu et al., 2016, 2014; Ma et al., 2018). Among these natural products, a chemically characterized and standardized pomegranate fruit extract (PE; commercially available as Pomella®), and its phenolic compounds, including punicalagin (PA) and ellagic acid (EA), along with their gut microbial metabolite, namely, urolithin A (UA), showed promising inhibitory effects on the formation of AGEs. Furthermore, mechanistic studies revealed that the anti-glycation activity of PE and PA is mediated by their potent MGO scavenging effects in a model system of bovine serum albumin (Liu et al., 2014). PE also showed anti-glycation effects by alleviating MGO induced protein mis-folding with a model of β-amyloid (Liu et al., 2016). In addition, PE and its phenolics exerted skin protective effects by reducing hydrogen peroxide (H_2O_2)-induced cytotoxicity and DNA damage in human keratinocyte HaCaT cells (Liu et al., 2019). However, it remains unknown whether PE and its phenolics can protect DNA integrity from RCS-induced oxidative stress and cell dysfunctions in HaCaT cells. Herein, we aimed to evaluate PE, and its phenolics, including PA, EA, and UA for: (1) DNA protective effects of against MGO-induced DNA damage in biochemical model and in cell based assays; and (2) skin protective effects against MGO-induced cytotoxicity, cellular ROS, and cell dysfunctions in human keratinocyte HaCaT cells.

2. Materials and methods

2.1. Materials and chemicals

A commercially available pomegranate extract (PE; Pomella®) was provided by Verdure Sciences (Noblesville, IN, USA). A voucher specimen (LPR4EP1703D15PS) has been deposited in the Heber W. Youngken Jr. Medicinal Garden Herbarium, College of Pharmacy, University of Rhode Island, USA. The phytochemical constituents of this PE have been extensively investigated by our group resulting in the identification of over seventy phytochemicals (Liu & Seeram, 2018; Yuan et al., 2016). PE was chemically standardized to its major phenolics including punicalagin (PA; c.a. 30%) and ellagic acid (EA; c.a. 2.3%), which were identified by HPLC analysis (Supplementary Materials Fig. S1). PA was purified from PE and urolithin A (UA) was synthesized by our group using previously reported methods (Yuan et al., 2016). Ellagic acid (EA), dimethyl sulfoxide (DMSO), methylglyoxal (MGO), 2′,7′-dichlorofluorescin diacetate (DCF-DA), Hoechst 33342, and crystal violet staining reagent were purchased from Sigma Chemical Co. (St. Louis, MO, USA). Dulbecco's modified Eagle's medium (DMEM) and fetal bovine serum (FBS) were purchased from Life Technologies (Gaithersburg, MD, USA). The CellTiter-Glo (CTG) kit was purchased from Promega (Fitchburg, WI, USA).

2.2. DNA oligonucleotide synthesis

Nine-mer single-stranded DNA oligonucleotide with the sequence 5′-TTTTGTTTT-3′ was synthesized by solid-phase phosphoramidite chemistry and purified by HPLC as previously described (Tang et al., 2017). Purification was carried out using an oligonucleotide anion-exchange column (DNAPac PA100; 4 × 250 mm, 13 μm; Thermo Fisher Scientific; Waltham, MA, USA) with two mobile phases including water (solvent A) and ammonium acetate in water (1.5 M; solvent B). Purified oligonucleotide was characterized by electrospray ionization time-of-flight mass spectrometry (ESI-TOF MS; AB Sciex; Framingham, MA, USA) and the concentration of oligonucleotides was determined by measuring UV absorbance at a wavelength of 260 nm on a NanoDrop spectrophotometer (Thermo Scientific 1000; Waltham, MA, USA).

2.3. Detection of MGO-DNA adducts by HPLC and mass spectrometry

Glycation reactions were performed in PBS buffer containing 9-mer oligonucleotide (200 μM) and MGO (200 μM) under physiological conditions (pH 7.4, 37 °C) for 7 days. LC-MS analysis was conducted on triple quadrupole-TOF 4600 mass spectrometer (AB Sciex; Framingham, MA, USA). ESI-MS was conducted under a negative ion mode by applying the following parameters: needle voltage at 4.5 kV, heater temperature at 300 °C, heater gas at 40 psi, nebulizer gas at 30 psi, curtain gas at 30 psi, declustering potential at −100 V, and the collision energy at −10 V. HPLC separation was achieved by using an Accucore 150 amide HILIC column (3 × 100 mm; 2.6 μm; Thermo Scientific; Waltham, MA, USA) at a flow rate of 0.3 mL/min with a solvent system of ammonium acetate (15 mM) in 90% aqueous acetonitrile (solvent A) and ammonium acetate (15 mM) in 10% aqueous acetonitrile (solvent B). A linear gradient was used as following condition: 30% of B for 5 min, 30–60% of B over 15 min, 60% of B over 5 min, 60–30% of B for 1 min and 30% of B over 15 min. The LC-MS data were analyzed by AB Sciex Analyst TF software 1.7..

2.4. Cell culture and viability assay

Human keratinocyte HaCaT cells were obtained from the American Type Culture Collection (Manassas, VA, USA) and maintained in DMEM supplemented with 5% FBS at 37 °C under an atmosphere of 5% CO_2 and 95% air. Cell viability was evaluated using the Cell Titer Glo2.0 assay (CTG 2.0) as previously reported (Ma, DaSilva, & et al., 2016). Test samples were prepared in DMSO and diluted to desired concentrations (6.25–200 μg/mL for PE and 6.25–200 μM for the pure compounds) with culture medium (DMSO < 0.1%). HaCaT cells were seeded at 5×10^4 cells/mL to yield 50–60% confluency in standard white-walled clear bottom 96-well plates and treated with PE and its phenolics for 24 h. Following an incubation period of 24 h, CTG 2.0 reagent was added in cell culture media (1:1 ratio) and mixed for 5 min on an orbital shaker, followed by measurement of the luminescence of each well using a plate reader (SpectraMax M2; Molecular Devices, Sunnyvale, CA, USA).

2.5. MGO induced cytotoxicity

Cytotoxicity of HaCaT cells induced by MGO (at 100, 200, 300, 400, 500, and 600 μM for 24 h) was measured by the CTG 2.0 assay as we previously reported (Liu et al., 2019).

2.6. Crystal violet and Hoechst staining

Morphological analysis of MGO-exposed HaCaT cells treated PE or its phenolics were visualized by staining reagents including crystal violet and Hoechst using protocols we previously reported (Liu et al., 2019).

2.7. Reactive oxygen species (ROS) assay

Generation of MGO-induced ROS in HaCaT cells were measured using a fluorescent probe DCF-DA with method we previously reported (Liu et al., 2019).

2.8. Comet assay

DNA structural integrity was evaluated by single-cell gel electrophoresis (the Comet assay) to measure the strand breaks in the DNA of

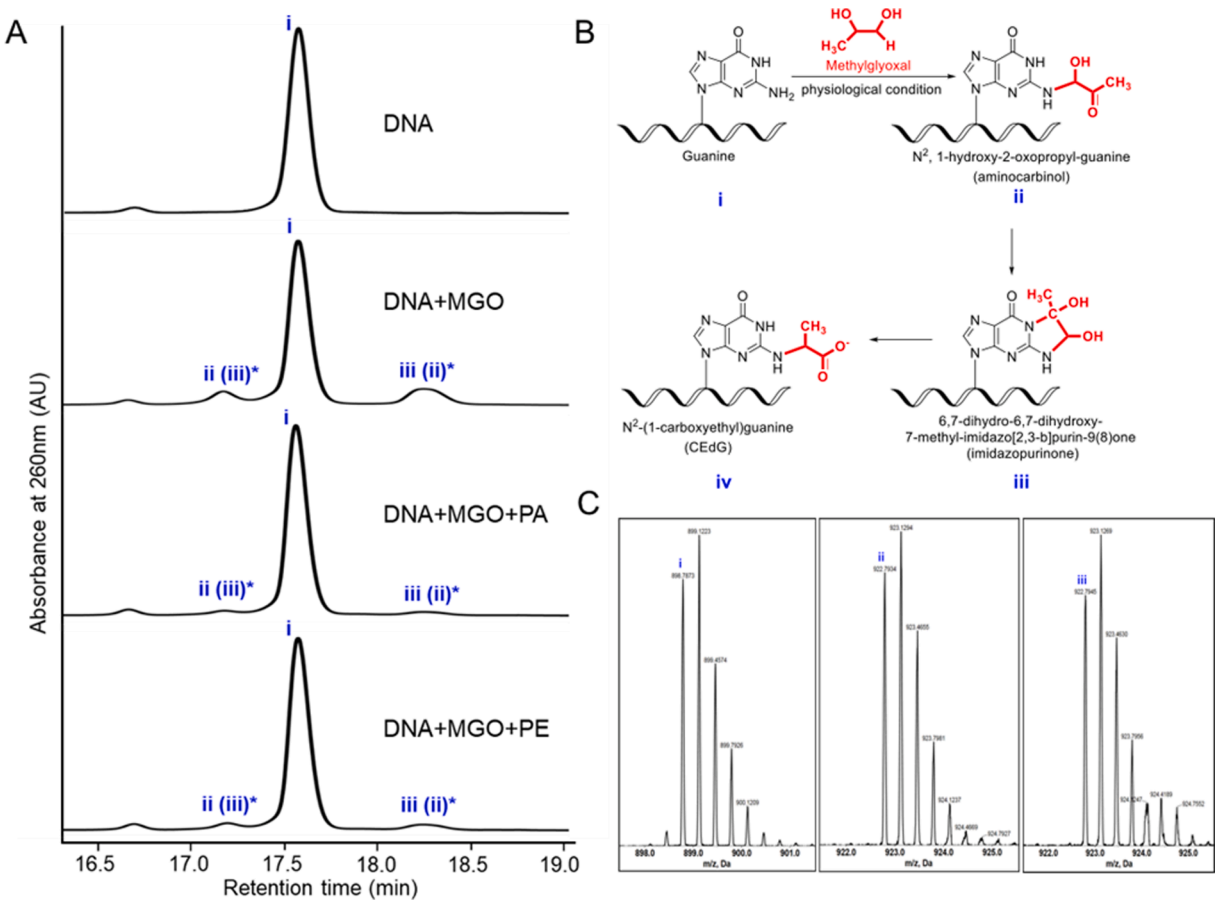

Fig. 1. Effects of PE and PA on the formation of MGO-induced DNA adducts. Representative HILIC-HPLC chromatograms of MGO-DNA adducts (formed at pH 7.4 and 37 °C for 7 days). A single MGO-reactive guanine nucleobase was incorporated in the defined oligonucleotide sequence and guanine reacts with MGO to form two intermediates: aminocarbinol (ii) and imidazopurinone (iii), and then converts into an advanced glycation endproduct (CEdG, iv). HPLC peaks represent intact 9mer single-stranded DNA oligonucleotide (i), and the MGO-DNA addcuts including aminocarbinol (ii), and imidazopurinone (iii) with a retention time of 17.6, 17.2, and 18.3 min, respectively (A). Scheme of the chemical reactions of the formation of MGO-DNA (B). High-resolution triple quadrupole-TOF MS analyses of guanine glycation products (C). Data represent their −3 charge envelopes with the observed *m/z* values of their monoisotopic at 898.79 (i), 922.79 (ii), and 922.79 (iii), matching their theoretical *m/z* at −3 charge are: 898.81 (i), 922.82 (ii), and 922.82 (iii) respectively. *arbitrarily assigned peak ii as aminocarbinol or peak iii as imidazopurinone based on their structural properties and retention. times in LC.

HaCaT cells using a Comet assay kit according to our previously reported method (Sheng et al., 2020).

2.9. Adhesion assay

Adhesion assay was conducted based on a previously reported method with minor modifications (Yang et al., 2014). Briefly, HaCaT cells were seeded at 5×10^4 cells/mL to yield 50–60% confluency in a 24-well plate and then pre-treated with test samples for 2 h. After the pre-treatment, cells were washed with PBS twice and then incubated with MGO (400 μM) for 24 h. Next, cells were then harvested and inoculated on two separate 96-well plates with 6 wells for each group in each plate. The CTG assay reagent was added to each experimental group (six wells) to measure the viability of total cells. The cells of each group in the other six wells were further cultured for 10 h, followed by removing the medium and washing with PBS twice to remove the unattached cells. Then the CTG 2.0 reagent was added to measure the viability of adhesive cells. The adhesion rate of cells was calculated by the viability of adhesive cells/total cells × 100%.

2.10. Cell migration transwell assay

Migration ability of HaCaT cells was measured by the transwell assay using previously reported method with minor modifications (Yang et al., 2014). Briefly, cells in 6-well plates were cultured to reach 80–90% confluency and then pretreated with test samples for 2 h followed by washing with PBS twice. Cells were then exposed to MGO (400 μM) for 24 h followed by digesting with trypsin and centrifuged at 300 *g* for 5 min. A cell suspension was obtained by suspending cells in serum free DMEM (2.5×10^5 cells/mL; 1 mL). Cell suspension (100 μL) was loaded into the upper compartment of the transwell chamber and incubated for 5 min. DMEM containing 5% FBS (600 μL) were added to a 24-well plate (the lower transwell chamber) and the cell suspension (300 μL) was added into the upper chamber. After 12 h incubation, cells in the upper chamber were washed with PBS and fixed with 75% ethanol for 15 min. Then cells in the upper chamber were stained with crystal violet staining reagent for 10 min and washed with PBS for 5 times and cells inside the upper chamber were removed by swab. Then cell images were taken with EVOS Cell Imaging System (Invitrogen, Waltham, MA, USA). Stained cells were then incubated in 75% ethanol for 15 min for decoloration and the optical density of the solution was recorded by a plate reader at a wavelength of 570 nm.

2.11. Scratch wound healing assay

An in vitro scratch wound healing assay was performed according to previously reported method with minor modifications (Yang et al., 2014). HaCaT cells were seeded in 6-well plates and cultured to reach

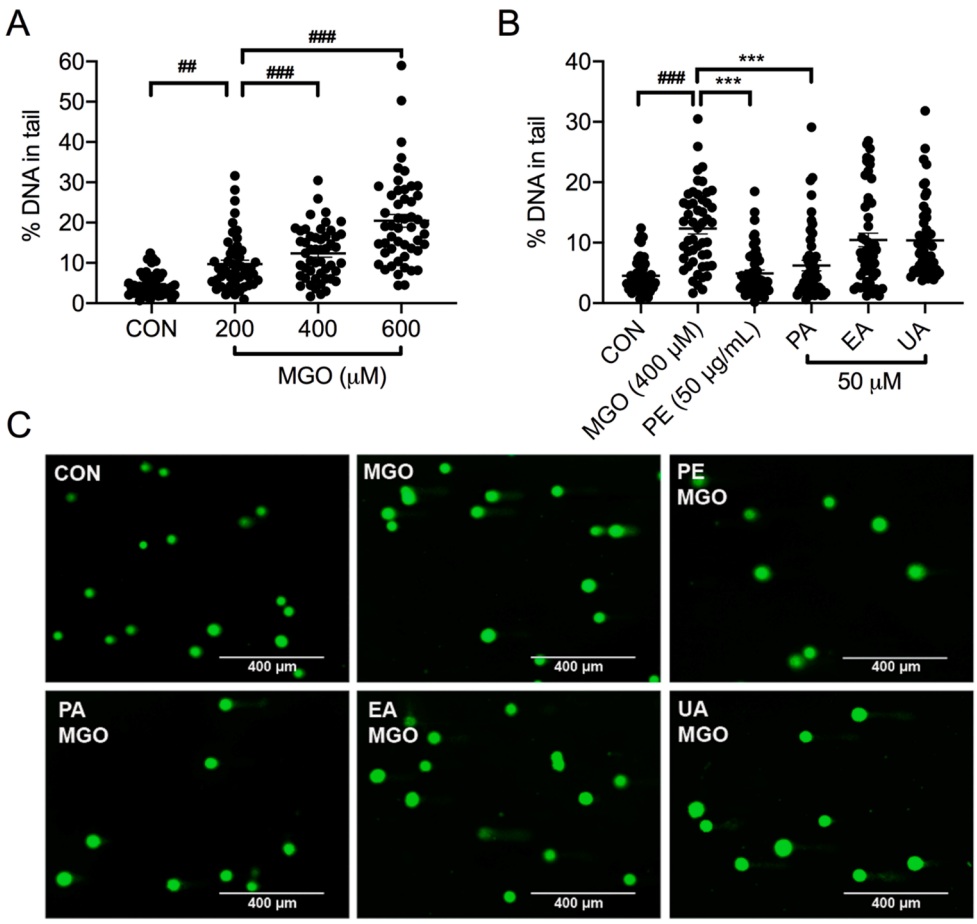

Fig. 2. Effects MGO (at 200, 400, and 600 μM) on the DNA integrity (as of % of DNA in tail) of HaCaT cells (A). Effects of PE (50 μg/mL) and its phenolic compounds including PA, EA, and UA (at 50 μM) on the DNA integrity (as of % of DNA in tail) of HaCaT treated challenged with MGO (400 μM; B). The percentage of tailed DNA were measured from randomly selected cells ($n > 50$) and analyzed with software CASP. Representative fluorescent images of SYBR GOLD stained Comet slides of HaCaT cells captured by an EVOS microscope system. Statistical significant difference was considered as $^{\#\#}p < 0.01$, $^{\#\#\#}p < 0.001$ and $^{\#\#\#\#}p < 0.0001$ when compared to the control group; and as $^{***}p < 0.001$ when compared to the MGO-treated group.

80–90% confluency followed by a pre-treatment with test samples for 2 h. After the treatments, a narrow wound-like gap in the cell monolayer was created with a pipette tip (1 mL size) in each well. The shedding cells were washed off with PBS and then the images were captured with an EVOS Cell Imaging System. The cells were further exposed to MGO (400 μM) for 48 h and the cell images were captured with EVOS Cell Imaging System. Gap area was quantitatively analyzed with the ImageJ (https://imagej.nih.gov/ij/) software and wound healing rate was calculated as [Gap area$_{(48h)}$ − Gap area$_{(0h)}$]/Gap area$_{(0h)}$ × 100%.

2.12. Statistical analysis

Data are expressed as the mean ± the standard error of the mean (S.E.M.). The significance of differences was determined using a two-way analysis of variance (ANOVA) followed by a post hoc Student-Newman–Keuls multiple comparison test (SNK). Differences were considered significant when $p < 0.05$.

3. Results and discussion

3.1. Pomegranate extract (PE) and punicalagin (PA) reduce the formation of DNA-MGO adducts

To evaluate the effect of MGO inducing DNA damages in vitro, we analyzed the formation of MGO-DNA adducts by incubating a 9mer single-stranded DNA oligonucleotide (5′-TTTTGTTTT-3′; 200 μM) with MGO (200 μM) under physiological conditions (pH 7.4 in PBS at 37 °C) for 7 days. To simplify the analysis of DNA adduct formation, a single MGO-reactive guanine nucleobase was incorporated in the defined oligonucleotide sequence. The starting material and reaction products were analyzed by using HPLC and LC-MS methods. The HPLC chromatograms of the reaction at the end point (Fig. 1A) showed a dominant peak (i; retention time at 17.6 min) representing the intact 9mer oligonucleotide, as well as two additional peaks (ii and iii; retention time of 17.2 and 18.3 min, respectively) after the DNA oligonucleotide was exposed to MGO. We further determined the molecular weight (MW) of the three peaks by LC-MS with m/z at 898.79 for i, 922.79 for ii, and 922.79 for iii at −3 charge state (Fig. 1B). These results were in agreement with previously reported data showing that MGO-DNA adducts including aminocarbinol and imidazopurinone (Fig. 1C) were the primarily products of MGO-induced guanine glycation (Richarme et al., 2017). Given that aminocarbinol and imidazopurinone have the same MW and cannot be distinguished by LC-MS, we arbitrarily assigned peak ii as aminocarbinol and peak iii as imidazopurinone based on their structural properties and retention times in the chromatogram (Fig. 1A and C). Next, we evaluated PE and its phenolics including PA, EA, and their gut microbial metabolite, UA, for their potential to reduce the formation of MGO-DNA adducts. Test samples (100 μg/mL for PE and 100 μM for PA, EA, and UA) were incubated with the 9mer oligonucleotide and MGO. Treatment of PE and PA reduced MGO-induced formation of peak ii and iii and with a reduction of peak area by 73.7 and 55.3%, respectively (Fig. 1A, and Table S1 in the Supplementary Materials). This suggested that PE and PA maintained the structure integrity of the DNA oligonucleotide by reducing the formation of aminocabinol and imidazopurinone DNA adducts.

The DNA protective effects of phytochemicals, such as curcumin from turmeric spice, against MGO-induced DNA damage are supported by data from gel electrophoresis experiments, but the MGO-DNA glycation adducts were not identified (Chan & Wu, 2006). Herein, a specific DNA single strand nucleotide, i.e. 5′-TTTTGTTTT-3, whose guanine but

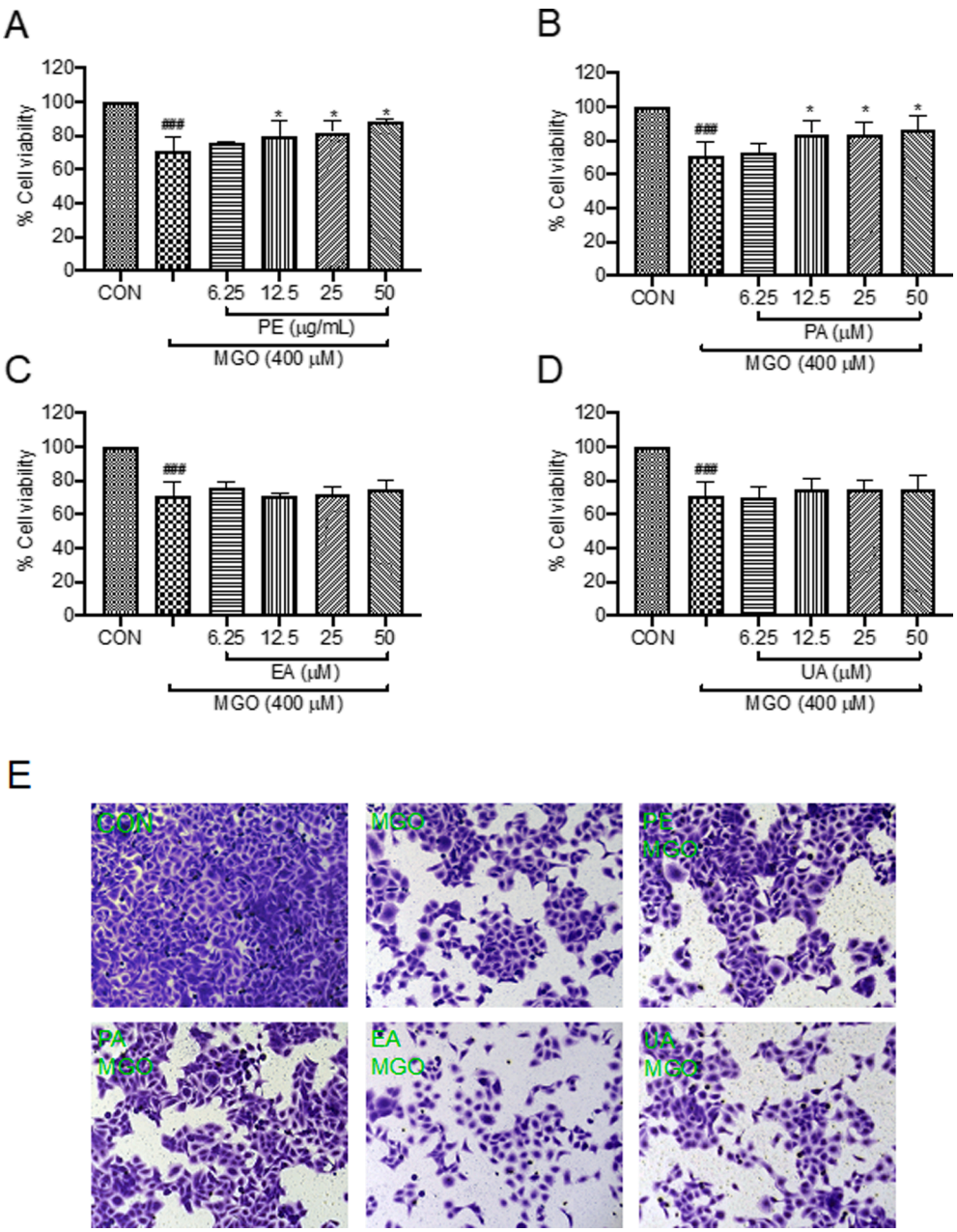

Fig. 3. Effects of PE and its phenolic compounds on the cell viability of MGO challenged HaCaT cells. Cells were pre-treated with PE (6.25, 12.5, 25, and 50 μg/mL; A) or PA, EA, and UA (6.25, 12.5, 25, and 50 μM; B-D, respectively) for 2 h, and then treated with MGO (400 μM) for 24 h. Cell viability was measured using the CTG 2.0 assay. Representative images of cells stained with crystal violet reagent [E; first row from left to right: control group; MGO (400 μM) model group; PE (50 μg/mL) + MGO (400 μM); second raw from left to right: PA (50 μM) + MGO (400 μM); EA (50 μM) + MGO (400 μM); and UA (50 μM) + MGO (400 μM)]. Statistical significant difference was considered as $^{###}p < 0.001$ when compared to the control group; and as $^{*}p < 0.05$ when compared to the MGO-treated group. (For interpretation of the references to colour in this figure legend, the reader is referred to the web version of this article.)

not thymine can react with MGO, was used as a simplified experimental model to measure the DNA-MGO adducts. This model enabled the detection of the DNA-MGO adducts using LC-MS analysis as the 9mer DNA single strand nucleotide has a preferable MW for the LC-MS measurements. To date, this is the first study showing that PE and PA protected DNA structural integrity against MGO-induced glycation by reducing specific MGO-DNA adducts including aminocarbinol and imidazopurinone, as elucidated by data from HPLC and LC-MS analysis. This protective effect may be attributed to PE and PA's anti-glycation and MGO scavenging activities as shown in our previously reported study (Liu et al., 2014). This effect was supported by the observation that other pomegranate phenolics including EA and UA with lower MGO trapping capacity had weaker protective effect on DNA integrity. In addition, it is possible that PE and its phenolics may also be involved in other mechanisms of DNA protection against MGO-induced glycation in living organisms. For instance, oxidative stress response proteins, such as protein deglycase (also known as DJ-1), can protect DNA from RCS-induced damage by repairing MGO-glycated nucleotides (Advedissian, Deshayes, Poirier, Viguier, & Richarme, 2016). However, the effects of PE and it phenolics on protein deglycase remain unclear warranting further studies to elucidate their mechanisms of action. Nevertheless, the findings from our current biochemical based experiments provide useful insights on the protective effects of PE and PA against MGO-induced DNA damage.

3.2. PE and its phenolics maintain DNA integrity against MGO-induced damage

To further evaluate the protective effects of PE and its phenolics against MGO-induced formation of DNA adducts in a living organism, a cell-based model with human keratinocytes HaCaT cells (Comet assay) was used to measure the effects of MGO-induced DNA damage. Exposure to MGO (200, 400, and 600 μM) impaired the DNA structural integrity of HaCaT cells and increased the level of tailed DNA by 2.16-, 2.74-, and 4.54-fold, respectively (Fig. 2 A). Treatment of PE (50 μg/mL) and PA (50 μM) protected HaCaT cellular DNA from MGO-induced damage by

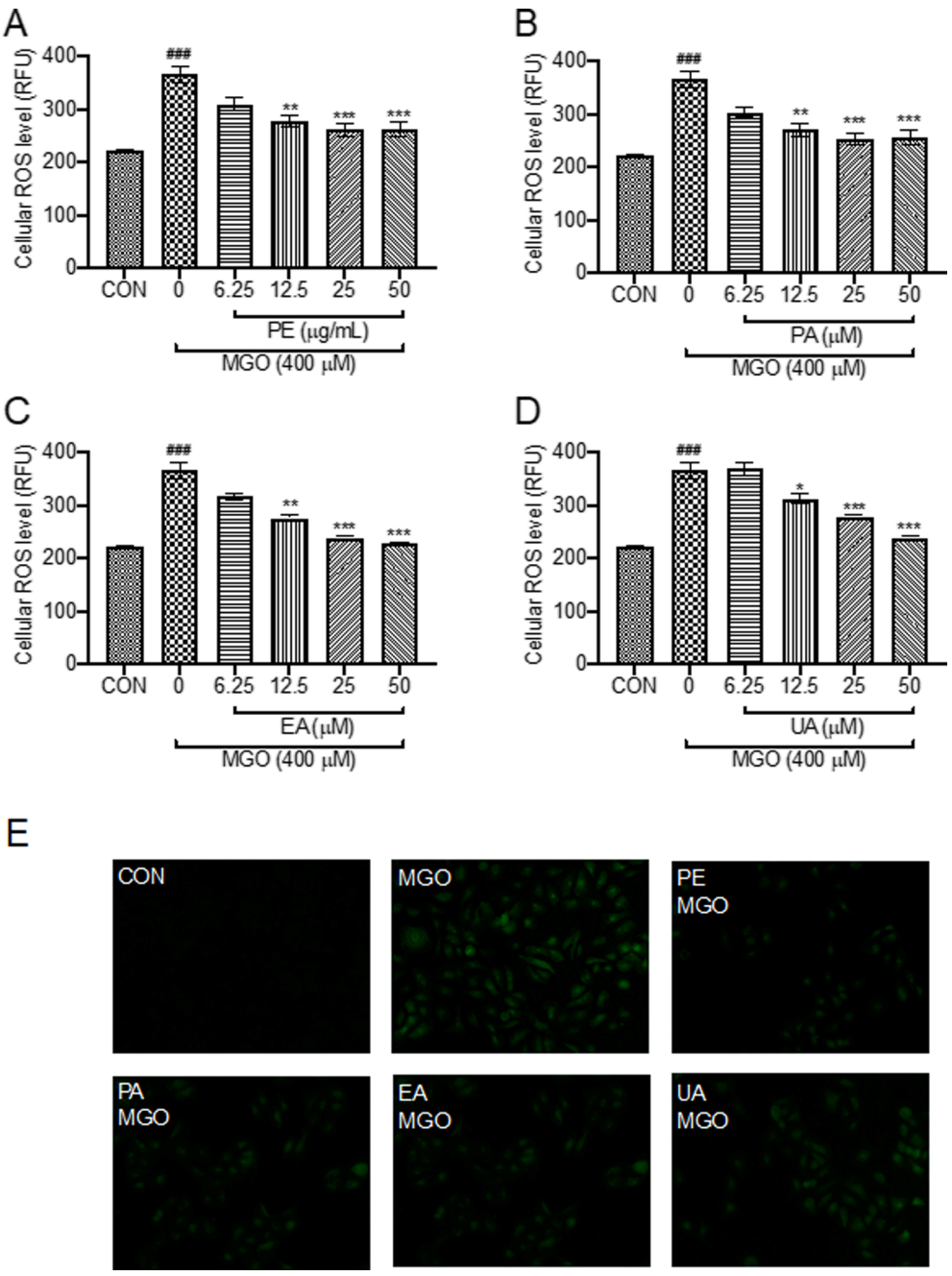

Fig. 4. Effects of PE and its phenolic compounds on the cellular ROS levels of MGO challenged HaCaT cells. Cells were pretreated with PE (6.25, 12.5, 25, and 50 μg/mL; A) or PA, EA, and UA (6.25, 12.5, 25, and 50 μM; B-D, respectively) for 2 h, and then treated with MGO (400 μM) for 24 h. ROS level was determined by measuring the fluorescent intensity of cells using the DCF-DA fluorescent probe. Representative fluorescent images of cells [E; first row from left to right: control group; MGO (400 μM) model group; PE (50 μg/mL) + MGO (400 μM); second raw from left to right: PA (50 μM) + MGO (400 μM); EA (50 μM) + MGO (400 μM); and UA (50 μM) + MGO (400 μM)]. Statistical significant difference was considered as $^{###}p < 0.001$ when compared to the control group; and as $^{*}p < 0.05$, $^{**}p < 0.01$, and $^{***}p < 0.001$ when compared to the MGO-treated group.

reducing tailed DNA by 60.2 and 49.7%, respectively (Fig. 2B), whilst EA and UA did not significantly decrease the level of tailed DNA. This protective effect was supported by the morphological analysis of HaCaT cells exposed to MGO which were then treated with PE or its phenolics. The immunofluorescent images of the nuclei of MGO-exposed cells were larger and brighter with irregular shapes as compared to the control group (Fig. S2 in Supplementary Materials), indicating that MGO indeed induced DNA damage in HaCaT cells. This detrimental effect was ameliorated by the treatment of PE (50 μg/mL), PA, EA and UA (all at 50 μM), which restored the regular shape of cell nuclei as shown in the Hoechst staining immunofluorescent images (Fig. 2C).

Data from cell-based assays further supported the protective effects of PE and PA against MGO-induced DNA damage. This is in agreement with a previously reported study showing that PE (Pomella®) protected human skin fibroblast cells against ultraviolet (UV)-induced DNA damage (Lisbeth, Noratto, Hingorani, Talcott, & Mertens-Talcott, 2008). Notably, although EA did not show significant protective effect in the Comet assay ($p = 0.59$), it has been reported that EA can alleviate UV-induced DNA damage by suppressing the production of ROS in HaCaT cells (Hseu et al., 2012). It is possible that PE's phenolics, such as EA, may have different defensive mechanisms when HaCaT cells exposed to different detrimental stimuli (i.e. RCS vs UV radiation). Furthermore, it is known that high level of cellular RCS triggers the overproduction of ROS, which leads to abnormal cell death (Liu et al., 2020). Therefore, we next evaluated the effects of PE and its phenolics on MGO-induced toxicity and oxidative stress in HaCaT cells.

3.3. PE and PA reduce MGO-induced toxicity in HaCaT cells

To evaluate the protective effects of PE and its phenolics against MGO-induced cellular damage in HaCaT cells, we assessed whether they could alleviate MGO-induced cytotoxicity. PE (3.13, 6.25, 12.5, 25, 50,

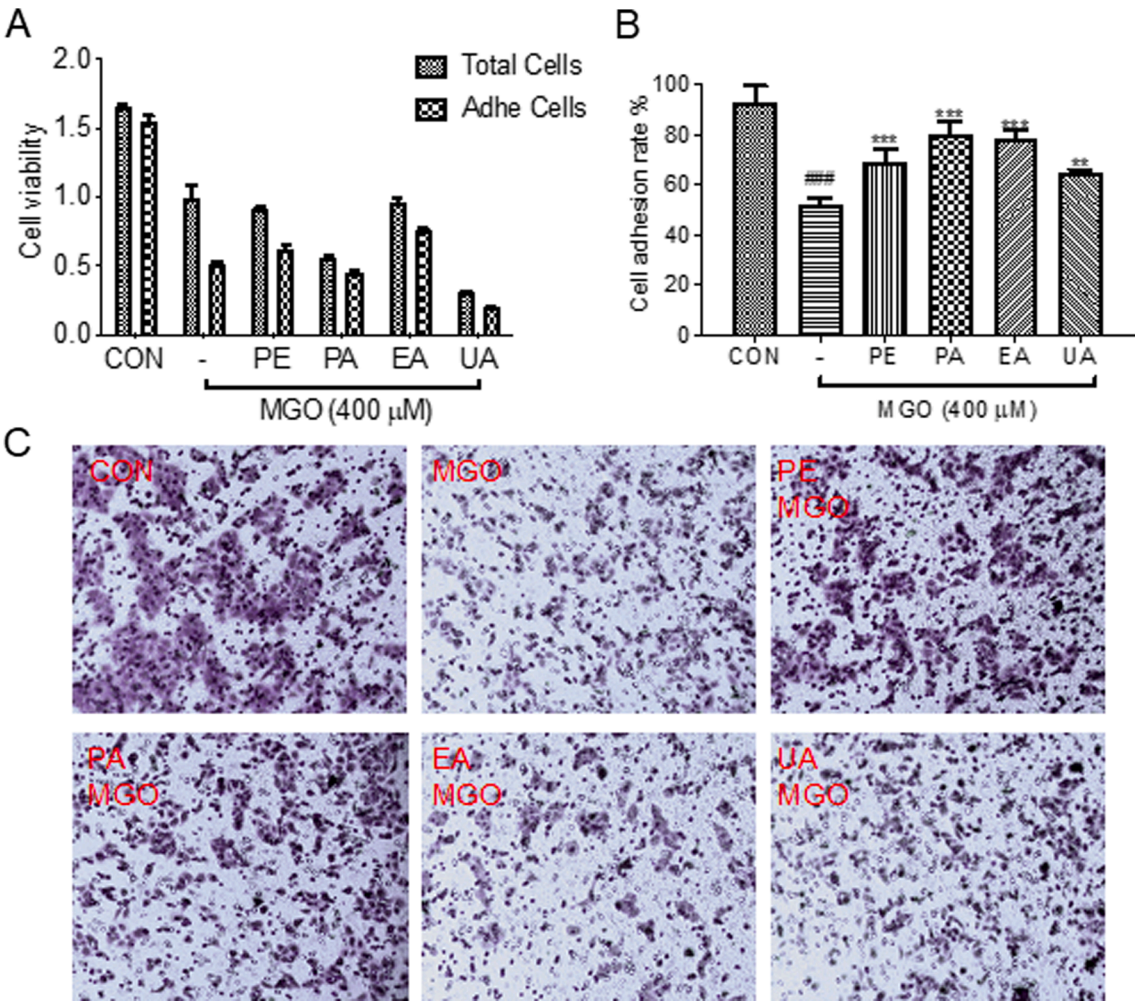

Fig. 5. Effects of PE and its phenolic compounds on the adhesion capacity of MGO challenged HaCaT cells. Cells were pre-treated with PE (50 μg/mL) or PA, EA, and UA (50 μM) for 2 h, and then treated with MGO (400 μM) for 24 h. Next, cell viability of total cells and adhesive cells was measured using the CTG assay (A) and the adhesion rate of cells was calculated by the viability of adhesive cells/total cells × 100% (B). Representative images of stained cells [C; first row from left to right: control group; MGO (400 μM) model group; PE (50 μg/mL) + MGO (400 μM); second raw from left to right: PA (50 μM) + MGO (400 μM); EA (50 μM) + MGO (400 μM); and UA (50 μM) + MGO (400 μM)]. Statistical significant difference was considered as, $^{###}p < 0.001$ when compared to the control group; and as $^{**}p < 0.01$ and $^{***}p < 0.001$ when compared to the MGO-treated group.

and 100 μg/mL) and its phenolics including PA, EA, and UA (3.13, 6.25, 12.5, 25, 50, and 100 μM) were non-toxic to HaCaT cells as they maintained cell viability (no<90%; Supplementary Materials Fig. S3). MGO (300, 400, 500, and 600 μM) induced cytotoxicity in HaCaT cells with cell viability reduced to 94.3, 74.9, 63.3, and 52.8%, respectively (Supplementary Materials Fig. S4) so MGO (400 μM) was subsequently used as a model of RCS-induced cellular damage for further assays. Treatment of PE (12.5, 25, and 50 μg/mL) and PA (12.5, 25, and 50 μM) alleviated MGO-induced cytotoxicity in HaCaT cells by increasing the cell viability by 4.2–17.5% and 1.8–15.0%, respectively, whilst EA and UA did not restore the cell viability (Fig. 3A-D). PE and PA's protective effects were supported by the morphological analysis of cells stained with crystal violet reagent, which showed that PE (50 μg/mL) and PA (50 μM) maintained the number of viable cells against MGO-induced cytotoxicity (Fig. 3E).

3.4. PE and its phenolics decrease MGO-induced reactive oxygen species (ROS) in HaCaT cells

The cytoprotective effects of PE and its phenolics may be attributed to their antioxidant effects in keratinocytes. Herein, we evaluated the antioxidant effects of PE, PA, EA and UA against MGO-induced oxidative stress in HaCaT cells. MGO at 200, 400, and 600 μM induced cellular oxidative stress and significantly increased the level of ROS by 33.0, 123.7, and 450.9%, respectively (Fig. S5 in Supplementary Materials). Treatment of PE (12.5, 25, and 50 μg/mL) and PA (12.5, 25, and 50 μM) reduced the levels of MGO-induced ROS by 15.7–28.3% and 17.3–29.9%, respectively (Fig. 4 A and B). EA and UA also showed antioxidant activity at a higher concentration (50 μM) and decreased the ROS level by 37.3 and 34.9%, respectively (Fig. 4 C and D).

PE and its phenolics protected HaCaT cells from MGO-induced toxicity and oxidative stress, which is in agreement with observations in our previously reported study showing that PE and its phenolics reduced H_2O_2-induced cell death and ROS (Liu et al., 2019). It is interesting that, apart from PA, only UA suppressed the stimulated production of ROS in both models of MGO- and H_2O_2-induced oxidative stress in HaCaT cells. This is not surprising as UA has been well studied in models of various cell lines for its antioxidant effects, which are associated with the regulation of numerous molecular pathways including phosphatidylinositol-3-kinase (PI3K)/AKT/mammalian target of rapamycin (mTOR) (Totiger et al., 2019). However, the molecular pathways that regulate the protective effects of PE, PA, and UA against MGO-induced oxidative stress in HaCaT cells were not examined here warranting further studies to elucidate their mechanisms of action.

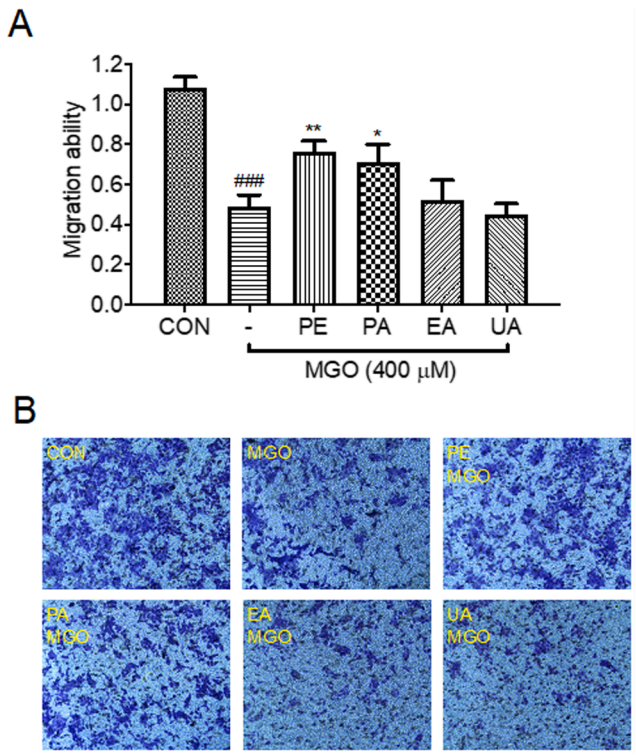

Fig. 6. Effects of PE and its phenolic compounds on the migration capacity of MGO challenged HaCaT cells. Cells were pre-treated with PE (50 μg/mL) or PA, EA, and UA (50 μM) for 2 h, and then treated with MGO (400 μM) for 24 h. The cell migration capacity of cells treated with each group was determined using the transwell assay (A). Representative microscopic images of cells [B; first row from left to right: control group; MGO (400 μM) model group; PE (50 μg/mL) + MGO (400 μM); second raw from left to right: PA (50 μM) + MGO (400 μM); EA (50 μM) + MGO (400 μM); and UA (50 μM) + MGO (400 μM)]. Statistical significant difference was considered as $^{###}p < 0.001$ when compared to the control group; and as $^{*}p < 0.05$ and $^{**}p < 0.01$ when compared to the MGO-treated group.

Nevertheless, this is the first study to show that UA, a gut microbial metabolite of PA, mitigated MGO-induced oxidative stress in HaCaT cells, which may also contribute to the overall skin protective effects of PE. To confirm the skin protective effects of PE and its phenolics, we evaluated their ameliorative effects against MGO-induced cell dysfunctions.

3.5. PE and its phenolics restore cellular adhesion and migration of MGO-exposed HaCaT cells

To further evaluate the protective effects of PE and its phenolics against MGO-induced cell damage, their effects on keratinocytes cellular functions including adhesion and migration were assessed. Exposure to MGO (400 μM) significantly impaired the adhesion ability of HaCaT cells resulting in reduced number of adhesive cells to 51.7% (Fig. 5A). Treatment by PE (50 μg/mL) and its phenolics, including PA, EA, and UA (all at 50 μM), restored the adhesion ability of HaCaT cells by 17.1, 28.2, 26.6, and 13.1%, respectively, as compared to the MGO-exposed cells (Fig. 5B and C). Cell migration function of HaCaT cells was also suppressed by MGO (400 μM) to 48.9% as compared to the control group (Fig. 6 A). Treatment of PE (50 μg/mL) and PA (50 μM) alleviated MGO-induced cell damage by increasing the migration function by 27.5 and 21.9%, respectively (Fig. 6A and B).

3.6. PE and PA enhance the wound healing ability of MGO-exposed HaCaT cells

Abnormal accumulation of AGEs and hyper-production of reactive carbonyl species are the major detrimental factors that contribute to diabetic complications such as skin ulcer (Schalkwijk & Stehouwer, 2020). The cytoprotective effects of PE and its phenolics against MGO-induced cellular dysfunction were further evaluated in a wound healing assay. Exposure to MGO (200, 400, and 600 μM) significantly impeded the course of wound healing and led to decreased healing rates (Fig. S6 in Supplementary Materials). The scratch closing process was hindered in the MGO-exposed group with a reduced wound healing rate by 72% as compared to the control group. Treatment by PE (50 μg/mL) and PA (50 μM) countered MGO-induced cell damage by enhancing the wound healing rate by 1.1- and 1.4-fold, respectively (Fig. 7 A and B). EA and UA did not show significant protective effects in the wound healing assay.

This is the first report on the protective effects of PE and its phenolics against MGO-induced cell dysfunctions including defected cell adhesion, migration, and wound healing abilities. These findings are in agreement with previously reported studies showing that PE and its phenolics can alleviate oxidative stress-induced damage in skin cells (Zaid, Afaq, Syed, Dreher, & Mukhtar, 2007). In addition, published in vivo studies support that PE can promote the wound healing process by the up-regulation of fibroblast infiltration, collagen regeneration, vascularization, and epithelialization (Yan et al., 2013) and by down-regulation of inflammatory neutrophil infiltration (Mo, Panichayupakaranant, Kaewnopparat, Nitiruangjaras, & Reanmongkol, 2014). It is possible that PE may also exert skin protective effects against MGO-induced oxidative stress via the aforementioned mechanisms given that PE has been reported to mediate collagen synthesis and exert anti-inflammatory effects in HaCaT cells (Park et al., 2018; Zaid et al., 2007). Additionally, published studies have shown that the wound healing effects of polyphenolic compounds from medicinal plants can be mediated by numerous signaling pathways, for instance, basic fibroblast growth factor (bFGF) and vascular endothelial growth factor (VEGF), as well as fibrosis-related genes including transforming growth factor-β (TGF-β) and α-smooth muscle actin (α-SMA) (Elbialy et al., 2021, 2020). While it is possible that pomegranate phenolics may also exert wound healing effects via the modulation of these signaling pathways, further molecular biology and in vivo studies are warranted to confirm this. These studies are critical for understanding PE's and its phenolics' mechanisms of action, which will provide critical information for their future development for potential biomedical applications. For instance, although polyphenolic compounds (being the major phytochemical constituents of PE) have shown various promising biological activities, their biomedical applications have been hampered due to limitations such as their poor bioavailability and challenging delivery routes (Agrawal, 2015; Chandra, Kumari, Bontempi, & Yadav, 2020). Therefore, further studies, including exploring different formulations, are warranted to address these challenges.

In the current study, using biochemical methods (nucleotides synthesis, HPLC, and MS) and cell-based assays (the Comet and Hoechst Staining), we revealed the protective effects of PE and PA against MGO induced DNA damage. In addition, their skin protective effects were characterized using assays measuring cell viability, cellular ROS, adhesion and migration, and wound healing capacity, which supported that PE and its phenolics can alleviate MGO-induced cell dysfunctions in HaCaT cells. However, several additional studies should be considered to elucidate the mechanisms of PE's and its phenolics' protective effects. First, molecular targets that play pivotal roles in the protection of HaCaT cells against RCS-induced oxidative stress should be identified. For instance, the effects of PE and its phenolics on proteins with detoxification functions, such as DJ-1 and glyoxalase I, remain to be evaluated. In addition, signaling pathways may be involved in the restoration of cell functions by PE and its phenolics and these should be examined.

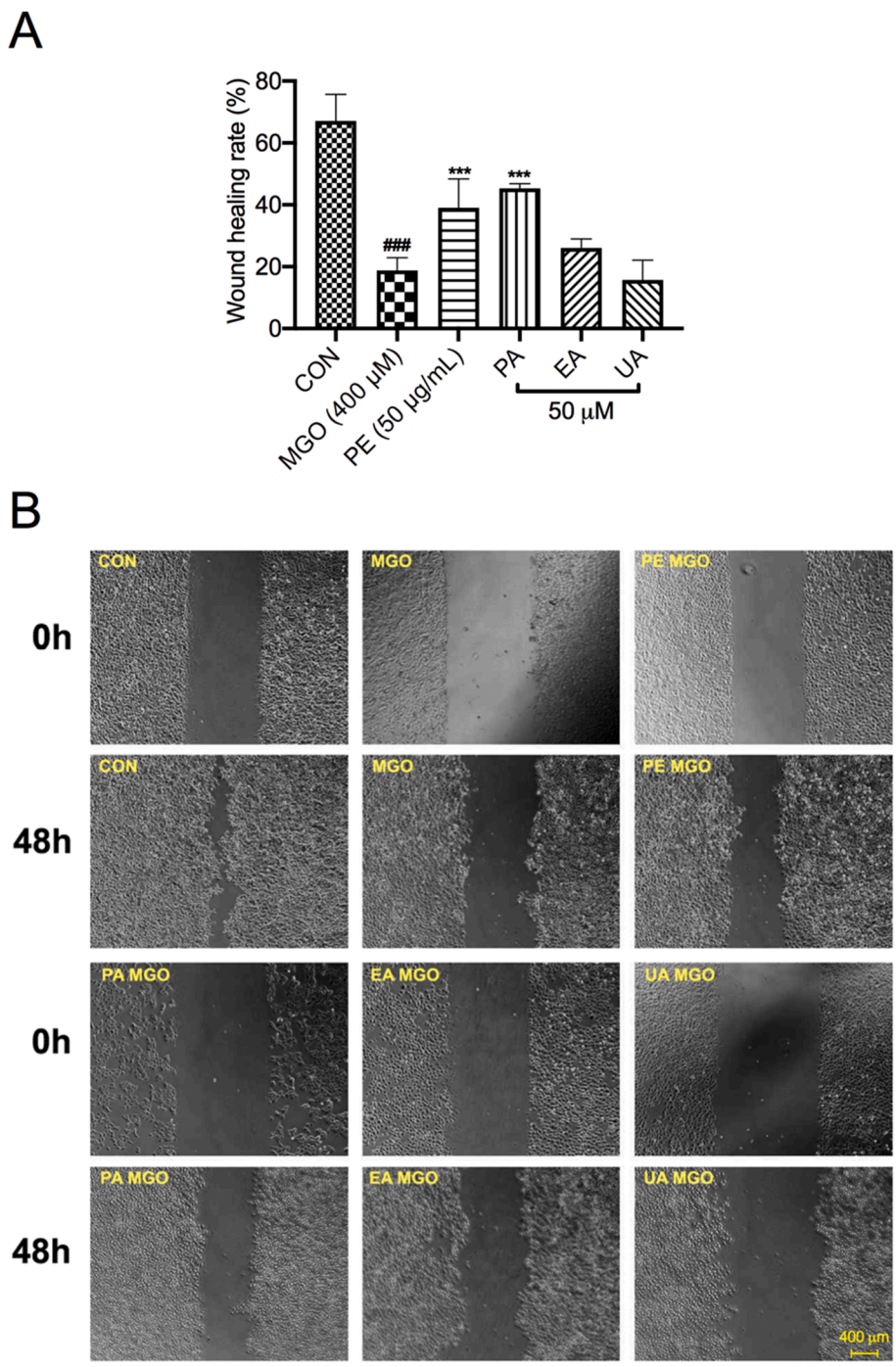

Fig. 7. Effects of PE and its phenolic compounds on the wound healing rate of MGO challenged HaCaT cells. Cells were pre-treated with PE (50 μg/mL) or PA, EA, and UA (50 μM) for 2 h, and then treated with MGO (400 μM) for 24 h. Next, a narrow wound-like gap in the cell plates was created with a pipette tips (1 mL size). Cells were washed off with PBS and the images were captured with an EVOS Cell Imaging System (0 h). Then cells were further exposed to MGO (400 μM) for 48 h and the cell images were captured with EVOS Cell Imaging System (48 h). Gap area was quantitatively analyzed with the ImageJ software and wound healing rate = [Gap Area(48 h)-Gap Area(0 h)]/Gap Area(0 h) × 100% (A). Representative microscopic images of cells [B; upper panel from left to right: control group at 0 and 48 h; MGO (400 μM) model group at 0 and 48 h; PE (50 μg/mL) + MGO (400 μM) at 0 and 48 h; lower panel from left to right: PA (50 μM) + MGO (400 μM) at 0 and 48 h; EA (50 μM) + MGO (400 μM) at 0 and 48 h; and UA (50 μM) + MGO (400 μM) at 0 and 48 h]. Statistical significant difference was considered as $^{###}p < 0.001$ when compared to the control group; and as $^{***}p < 0.001$ when compared to the MGO-treated group.

Nevertheless, the findings from our current study provide useful insights on the protective effects of PE and its phenolics on DNA and skin keratinocytes supporting their potential applications as bioactive ingredients for cosmeceuticals.

4. Conclusion

In summary, a standardized PE and its phenolics PA, EA, and their gut microbial metabolite, UA, were evaluated for DNA protective effects against MGO induced damage. PE and PA reduced the formation of MGO-DNA adducts and protected DNA integrity of HaCaT cells. In addition, PE and its phenolics protected HaCaT cells by alleviating MGO-induced cytotoxicity and cellular oxidative stress. The cytoprotective effects of PE and its phenolics were further supported by their activities observed in the cell adhesion and migration, as well as wound healing assays. Findings from this study delineate the protective effects of PE and its phenolics on DNA integrity and human keratinocytes against MGO-induced oxidative stress. Further studies on the mechanisms of action, including identifying the molecular targets, are warranted to support the application of PE and its bioactive phenolics for cosmeceuticals.

Funding

H.G. was supported by funding from China Scholarship Council (201708210229) and NSFC (81903228 HG).

CRediT authorship contribution statement

Hao Guo: Conceptualization, Methodology, Data curation, Writing - original draft, Funding acquisition. **Chang Liu:** Methodology, Data curation, Writing - original draft. **Qi Tang:** Methodology, Data curation, Writing - original draft. **Deyu Li:** Methodology, Writing - review & editing, Supervision. **Yinsheng Wan:** Methodology, Writing - review & editing, Supervision. **Jiu-Hong Li:** Writing - review & editing. **Xing-Hua Gao:** Writing - review & editing. **Navindra P. Seeram:** Writing - review & editing. **Hang Ma:** Conceptualization, Writing - review & editing, Supervision. **Hong-Duo Chen:** Writing - review & editing.

Acknowledgments

Data were acquired from instruments located at the University of Rhode Island in the RI-INBRE core facility obtained from Grant P20GM103430 from the National Center for Research Resources (NCRR), a component of the National Institutes of Health (NIH). The plant material was kindly provided by Mr. Ajay Patel, Verdure Sciences (Noblesville, IN, USA).

Declaration of Competing Interest

The authors declare that they have no known competing financial interests or personal relationships that could have appeared to influence the work reported in this paper.

Appendix A. Supplementary material

Supplementary data to this article can be found online at https://doi.org/10.1016/j.jff.2021.104564.

References

Advedissian, T., Deshayes, F., Poirier, F., Viguier, M., & Richarme, G. (2016). The Parkinsonism-associated protein DJ-1/Park7 prevents glycation damage in human keratinocyte. *Biochemical and Biophysical Research Communications, 473*(1), 87–91. https://doi.org/10.1016/j.bbrc.2016.03.056.

Agrawal, M. (2015). Natural polyphenols based new therapeutic avenues for advanced biomedical applications. *Drug Metabolism Reviews*. https://doi.org/10.3109/03602532.2015.1102933.

Chan, W. H., & Wu, H. J. (2006). Protective effects of curcumin on methylglyoxal-induced oxidative DNA damage and cell injury in human mononuclear cells. *Acta Pharmacologica Sinica, 27*(9), 1192–1198. https://doi.org/10.1111/j.1745-7254.2006.00374.x.

Chandra, H., Kumari, P., Bontempi, E., & Yadav, S. (2020). Medicinal plants: Treasure trove for green synthesis of metallic nanoparticles and their biomedical applications. *Biocatalysis and Agricultural Biotechnology*. https://doi.org/10.1016/j.bcab.2020.101518.

Elbialy, Z. I., Assar, D. H., Abdelnaby, A., Asa, S. A., Abdelhiee, E. Y., Ibrahim, S. S., … Atiba, A. (2021). Healing potential of Spirulina platensis for skin wounds by modulating bFGF, VEGF, TGF-ß1 and α-SMA genes expression targeting angiogenesis and scar tissue formation in the rat model. *Biomedicine and Pharmacotherapy, 137*, 111349. https://doi.org/10.1016/j.biopha.2021.111349.

Elbialy, Z. I., Atiba, A., Abdelnaby, A., Al-Hawary, I. I., Elsheshtawy, A., El-Serehy, H. A., … Assar, D. H. (2020). Collagen extract obtained from Nile tilapia (*Oreochromis niloticus* L.) skin accelerates wound healing in rat model via up regulating VEGF, bFGF, and α-SMA genes expression. *BMC Veterinary Research, 16*(1), 352. https://doi.org/10.1186/s12917-020-02566-2.

Hseu, Y. C., Chou, C. W., Senthil Kumar, K. J., Fu, K. T., Wang, H. M., Hsu, L. S., … Yang, H. L. (2012). Ellagic acid protects human keratinocyte (HaCaT) cells against UVA-induced oxidative stress and apoptosis through the upregulation of the HO-1 and Nrf-2 antioxidant genes. *Food and Chemical Toxicology, 50*(5), 1245–1255. https://doi.org/10.1016/j.fct.2012.02.020.

Kumagai, Y., Nakatani, S., Onodera, H., Nagatomo, A., Nishida, N., Matsuura, Y., … Wada, M. (2015). Anti-glycation effects of pomegranate (*Punica granatum* L.) fruit extract and its components in vivo and in vitro. *Journal of Agricultural and Food Chemistry, 63*(35), 7760–7764. https://doi.org/10.1021/acs.jafc.5b02766.

Kusirisin, W., Srichairatanakool, S., Lerttrakarnnon, P., Lailerd, N., Suttajit, M., Jaikang, C., & Chaiyasut, C. (2009). Antioxidative activity, polyphenolic content and anti-glycation effect of some thai medicinal plants traditionally used in diabetic patients. *Medicinal Chemistry, 5*(2), 139–147. https://doi.org/10.2174/157340609787582918.

Lisbeth, A., Noratto, G., Hingorani, L., Talcott, S. T., & Mertens-Talcott, S. U. (2008). Protective effects of standardized pomegranate (*Punica granatum* L.) polyphenolic extract in ultraviolet-irradiated human skin fibroblasts. *Journal of Agricultural and Food Chemistry, 56*(18), 8434–8441. https://doi.org/10.1021/jf8005307.

Liu, C., Guo, H., Dain, J. A., Wan, Y., Gao, X. H., Chen, H. D., … Ma, H. (2020). Cytoprotective effects of a proprietary red maple leaf extract and its major polyphenol, ginnalin A, against hydrogen peroxide and methylglyoxal induced oxidative stress in human keratinocytes. *Food & Function, 11*(6), 5105–5114. https://doi.org/10.1039/d0fo00359j.

Liu, C., Guo, H., DaSilva, N. A., Li, D., Zhang, K., Wan, Y., … Ma, H. (2019). Pomegranate (*Punica granatum*) phenolics ameliorate hydrogen peroxide-induced oxidative stress and cytotoxicity in human keratinocytes. *Journal of Functional Foods, 54*, 559–567. https://doi.org/10.1016/j.jff.2019.02.015.

Liu, W., Cai, A., Carley, R., Rocchio, R., Petrovas, Z. M., Chartier, C. A., … Seeram, N. P. (2018). Bioactive anthraquinones found in plant foods interact with human serum albumin and inhibit the formation of advanced glycation endproducts. *Journal of Food Bioactives, 4*, 130–138.

Liu, W., Ma, H., DaSilva, N. A., Rose, K. N., Johnson, S. L., Zhang, L., … Seeram, N. P. (2016). Development of a neuroprotective potential algorithm for medicinal plants. *Neurochemistry International, 100*, 164–177. https://doi.org/10.1016/j.neuint.2016.09.014.

Liu, W., Ma, H., Frost, L., Yuan, T., Dain, J. A., & Seeram, N. P. (2014). Pomegranate phenolics inhibit formation of advanced glycation endproducts by scavenging reactive carbonyl species. *Food and Function, 5*(11), 2996–3004. https://doi.org/10.1039/c4fo00538d.

Liu, W., Wei, Z., Ma, H., Cai, A., Liu, Y., Sun, J., … Seeram, N. P. (2017). Anti-glycation and anti-oxidative effects of a phenolic-enriched maple syrup extract and its protective effects on normal human colon cells. *Food and Function, 8*(2), 757–766. https://doi.org/10.1039/c6fo01360k.

Liu, Y., & Seeram, N. P. (2018). Liquid chromatography coupled with time-of-flight tandem mass spectrometry for comprehensive phenolic characterization of pomegranate fruit and flower extracts used as ingredients in botanical dietary supplements. *Journal of Separation Science, 41*(15), 3022–3033. https://doi.org/10.1002/jssc.201800480.

Ma, H., DaSilva, N. A., Liu, W., Nahar, P. P., Wei, Z., Liu, Y., … Seeram, N. P. (2016). Effects of a standardized phenolic-enriched maple syrup extract on β-amyloid aggregation, neuroinflammation in microglial and neuronal cells, and β-amyloid induced neurotoxicity in *Caenorhabditis elegans*. *Neurochemical Research, 41*(11), 2836–2847. https://doi.org/10.1007/s11064-016-1998-6.

Ma, H., Johnson, S. L., Liu, W., Dasilva, N. A., Meschwitz, S., Dain, J. A., & Seeram, N. P. (2018). Evaluation of polyphenol anthocyanin-enriched extracts of blackberry, black raspberry, blueberry, cranberry, red raspberry, and strawberry for free radical scavenging, reactive carbonyl species trapping, anti-glycation, anti-β-amyloid aggregation, and microglial neuroprotective effects. *International Journal of Molecular Sciences, 19*(2). https://doi.org/10.3390/ijms19020461.

Ma, H., Liu, W., Frost, L., Kirschenbaum, L. J., Dain, J. A., & Seeram, N. P. (2016). Glucitol-core containing gallotannins inhibit the formation of advanced glycation end-products mediated by their antioxidant potential. *Food and Function, 7*(5), 2213–2222. https://doi.org/10.1039/c6fo00169f.

Ma, H., Liu, W., Frost, L., Wang, L., Kong, L., Dain, J. A., & Seeram, N. P. (2015). The hydrolyzable gallotannin, penta-O-galloyl-β-d-glucopyranoside, inhibits the formation of advanced glycation endproducts by protecting protein structure. *Molecular BioSystems, 11*(5), 1338–1347. https://doi.org/10.1039/c4mb00722k.

Mano, J. (2012). Reactive carbonyl species: Their production from lipid peroxides, action in environmental stress, and the detoxification mechanism. *Plant Physiology and Biochemistry, 59*, 90–97. https://doi.org/10.1016/j.plaphy.2012.03.010.

Mo, J., Panichayupakaranant, P., Kaewnopparat, N., Nitiruangjaras, A., & Reanmongkol, W. (2014). Wound healing activities of standardized pomegranate rind extract and its major antioxidant ellagic acid in rat dermal wounds. *Journal of Natural Medicines, 68*(2), 377–386. https://doi.org/10.1007/s11418-013-0813-9.

Murata-Kamiya, N., & Kamiya, H. (2001). Methylglyoxal, and endogenous aldehyde, crosslinks DNA polymerase and the substrate DNA. *Nucleic Acids Research, 29*(16), 3433–3438. https://doi.org/10.1093/nar/29.16.3433.

Park, E. K., Lee, H. J., Lee, H., Kim, J. H., Hwang, J., Koo, J. Il, & Kim, S. H. (2018). The anti-wrinkle mechanism of melatonin in UVB treated HaCaT keratinocytes and hairless mice via inhibition of ROS and sonic hedgehog mediated inflammatory proteins. *International Journal of Molecular Sciences, 19*(7), 1995. https://doi.org/10.3390/ijms19071995.

Ramkissoon, J. S., Mahomoodally, M. F., Ahmed, N., & Subratty, A. H. (2013). Antioxidant and anti-glycation activities correlates with phenolic composition of tropical medicinal herbs. *Asian Pacific Journal of Tropical Medicine, 6*(7), 561–569. https://doi.org/10.1016/S1995-7645(13)60097-8.

Richarme, G., Liu, C., Mihoub, M., Abdallah, J., Leger, T., Joly, N., … Lamouri, A. (2017). Guanine glycation repair by DJ-1/Park7 and its bacterial homologs. *Science, 357*(6347), 208–211. https://doi.org/10.1126/science.aag1095.

Schalkwijk, C. G., & Stehouwer, C. D. A. (2020). Methylglyoxal, a highly reactive dicarbonyl compound, in diabetes, its vascular complications, and other age-related diseases. *Physiological Reviews, 100*(1), 407–461. https://doi.org/10.1152/physrev.00001.2019.

Semchyshyn, H. M. (2014). Reactive carbonyl species in vivo: Generation and dual biological effects. *The Scientific World Journal, 2014*. https://doi.org/10.1155/2014/417842.

Sheng, J., Liu, C., Petrovas, S., Wan, Y., Chen, H. D., Seeram, N. P., & Ma, H. (2020). Phenolic-enriched maple syrup extract protects human keratinocytes against hydrogen peroxide and methylglyoxal induced cytotoxicity. *Dermatologic Therapy, 33*(3). https://doi.org/10.1111/dth.13426.

Singh, R., Barden, A., Mori, T., & Beilin, L. (2001). Advanced glycation end-products: A review. *Diabetologia, 44*, 129–146. https://doi.org/10.1007/s001250051591.

Sun, J., Liu, W., Ma, H., Marais, J. P. J., Khoo, C., Dain, J. A., … Seeram, N. P. (2016). Effect of cranberry (*Vaccinium macrocarpon*) oligosaccharides on the formation of advanced glycation end-products. *Journal of Berry Research, 6*(2), 149–158. https://doi.org/10.3233/JBR-160126.

Tang, Q., Cai, A., Bian, K., Chen, F., Delaney, J. C., Adusumalli, S., … Li, D. (2017). Characterization of byproducts from chemical syntheses of oligonucleotides containing 1-methyladenine and 3-methylcytosine. *ACS Omega, 2*(11), 8205–8212. https://doi.org/10.1021/acsomega.7b01482.

Totiger, T. M., Srinivasan, S., Jala, V. R., Lamichhane, P., Dosch, A. R., Gaidarski, A. A., … Nagathihalli, N. S. (2019). Urolithin A, a novel natural compound to target PI3K/AKT/mTOR pathway in pancreatic cancer. *Molecular Cancer Therapeutics, 18*(2), 301–311. https://doi.org/10.1158/1535-7163.MCT-18-0464.

Yan, H., Peng, K. J., Wang, Q. L., Gu, Z. Y., Lu, Y. Q., Zhao, J., … Wang, X. C. (2013). Effect of pomegranate peel polyphenol gel on cutaneous wound healing in alloxan-induced diabetic rats. *Chinese Medical Journal, 126*(9), 1700–1706. https://doi.org/10.3760/cma.j.issn.0366-6999.20122728.

Yang, C. T., Zhao, Y., Xian, M., Li, J. H., Dong, Q., Bai, H. B., … Zhang, M. F. (2014). A novel controllable hydrogen sulfide-releasing molecule protects human skin keratinocytes against methylglyoxal-induced injury and dysfunction. *Cellular Physiology and Biochemistry, 34*(4), 1304–1317. https://doi.org/10.1159/000366339.

Yuan, T., Ma, H., Liu, W., Niesen, D. B., Shah, N., Crews, R., … Seeram, N. P. (2016). Pomegranate's neuroprotective effects against Alzheimer's disease are mediated by urolithins, its ellagitannin-gut microbial derived metabolites. *ACS Chemical Neuroscience, 7*(1), 26–33. https://doi.org/10.1021/acschemneuro.5b00260.

Zaid, M. A., Afaq, F., Syed, D. N., Dreher, M., & Mukhtar, H. (2007). Inhibition of UVB-mediated oxidative stress and markers of photoaging in immortalized HaCaT keratinocytes by pomegranate polyphenol extract POMx. *Photochemistry and Photobiology, 83*(4), 882–888. https://doi.org/10.1111/j.1751-1097.2007.00157.x.

Zhang, Y., Ma, H., Liu, W., Yuan, T., & Seeram, N. P. (2015). New antiglycative compounds from cumin (*Cuminum cyminum*) spice. *Journal of Agricultural and Food Chemistry, 63*(46), 10097–10102. https://doi.org/10.1021/acs.jafc.5b04796.